Molecular-Scale and Wide-Energy-Range Tunneling Spectroscopy on Self-Assembled Monolayers of Alkanethiol Molecules

Masato Nakaya,[†,‡] Masaya Shikishima,[‡] Masahiro Shibuta,[†,‡] Naoyuki Hirata,[†,‡] Toyoaki Eguchi,[†,‡] and Atsushi Nakajima[†,‡,*]

[†]Nakajima Designer Nanocluster Assembly Project, ERATO, JST, KSP, 3-2-1 Sakado, Takatsu-ku, Kawasaki 213-0012, Japan and [‡]Department of Chemistry, Faculty of Science and Technology, Keio University, 3-14-1 Hiyoshi, Kohoku-ku, Yokohama 223-8522, Japan

ABSTRACT

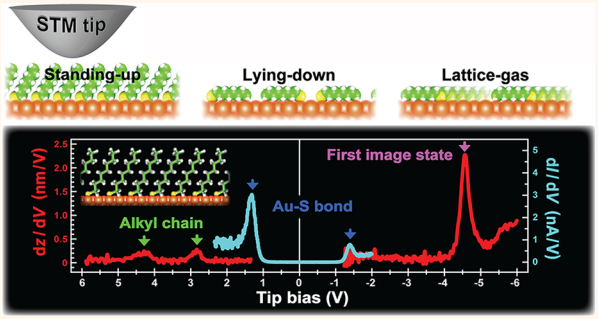

The electronic properties of alkanethiol self-assembled monolayers (alkanethiolate SAMs) associated with their molecular-scale geometry are investigated using scanning tunneling microscopy and spectroscopy (STM/STS). We have selectively formed the three types of alkanethiolate SAMs with standing-up, lying-down, and lattice-gas phases by precise thermal annealing of the SAMs which are conventionally prepared by depositing alkanethiol molecules onto Au(111) surface in solution. The empty and filled states of each SAM are evaluated over a wide energy range covering 6 eV above/below the Fermi level (E_F) using two types of STS on the basis of tunneling current—voltage and distance—voltage measurements. Electronic states originating from rigid covalent bonds between the thiol group and substrate surface are observed near E_F in the standing-up and lying-down phases but not in the lattice-gas phase. These states contribute to electrical conduction in the tunneling junction at a low bias voltage. At a higher energy, a highly conductive state stemming from the alkyl chain and an image potential state (IPS) formed in a vacuum gap appear in all phases. The IPS shifts toward a higher energy through the change in the geometry of the SAM from the standing-up phase to the lattice-gas phase through the lying-down phase. This is explained by the increasing work function of alkanethiolate/Au(111) with decreasing density of surface molecules.

KEYWORDS: alkanethiol · self-assembled monolayer · scanning tunneling microscopy · scanning tunneling spectroscopy · image potential state

The realization of practical nanoelectronics composed of well-controlled metal/molecule/metal junctions, which combine sophisticated functions such as electrical switching, energy conversion, charge storage, and physical/chemical sensing, has been one of the goals in recent molecular science and technology.[1−3] The key technology toward achieving this end is the controlled assembly of predesigned molecular building blocks into functional hierarchical structures on metal surfaces.[4,5] As promising candidates for the molecular building block, self-assembled monolayers (SAMs) of alkanethiols or their derivatives have been extensively studied owing to their ease of preparation[6−10] and versatility for functionalization *via* modification of the terminal group.[11−14]

Despite the diversity of investigated systems, several fundamental aspects of their electrical and electronic properties remain controversial. For example, there is a large discrepancy between the average tunneling barrier of a charged carrier, which ranges from 1.3 to 2.7 eV, extracted from conductivity measurements by making metal/molecule/metal junctions,[15−17] and the barrier expected from the energy difference between the Fermi level (E_F) and the highest occupied molecular orbital (HOMO) of an alkanethiolate SAM (~5 eV), as found by ultraviolet photoelectron spectroscopy (UPS).[18] To the best of our knowledge of the electrical and electronic properties of alkanethiolate SAMs on metal surfaces, these properties should be evaluated together with their molecular-scale geometry, because there is a large variety of molecular orientations and packing structures in the SAMs depending on the environmental temperature, molecular density, molecule−substrate interaction, and so forth.[6−10,19−23] In addition, it is also necessary to elucidate the empty and filled states of the SAMs over a wide energy range, because it has been theoretically predicted that the characteristic electronic states derived from the thiol

* Address correspondence to nakajima@chem.keio.ac.jp.

Received for review May 31, 2012 and accepted September 3, 2012.

Published online September 07, 2012
10.1021/nn302405r

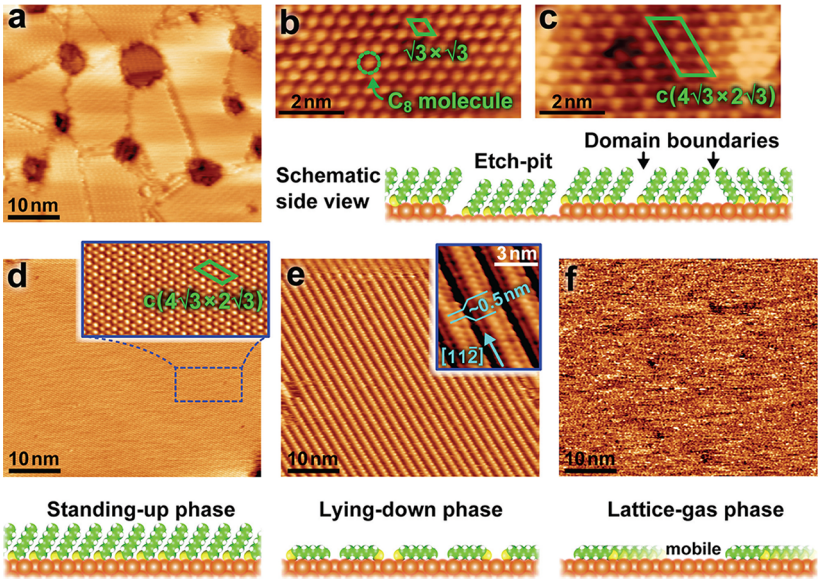

Figure 1. Control of geometry of C_8-SAMs by thermal annealing. (a) STM image (V_{tip} = 0.9 V and I_t = 2 pA) of a C_8-SAM formed in a solution. (b and c) High-resolution images (V_{tip} = 1.2 V and I_t = 5 pA) taken on each domain of the SAM with $\sqrt{3} \times \sqrt{3}$ and c($4\sqrt{3} \times 2\sqrt{3}$) superstructures, respectively. (d, e, f) STM images (V_{tip} = −1.0 V and I_t = 5 pA) taken on the C_8-SAM after annealing in UHV at 70, 120, and 150 °C, respectively. The insets in panels d and e are high-resolution images.

group, alkyl chain, and end group of alkanethiol are located at approximately 1−6 eV below/above E_F.[24−26] These states are related to the conduction, injection, and storage of charged carriers in the SAMs.

In this study, we have investigated the geometric and electronic structures of alkanethiolate SAMs formed on Au(111) surfaces at the molecular scale using scanning tunneling microscopy and spectroscopy (STM/STS). We mainly used SAMs of octanethiol molecules [$CH_3(CH_2)_7SH$, referred to as C_8 molecules hereafter] as samples (see Experimental Methods), which were prepared by depositing C_8 molecules onto Au(111) surfaces from the liquid phase. The geometry of each SAM was controlled from the standing-up phase to the lattice-gas phase through the lying-down phase by thermal annealing in an ultrahigh vacuum (UHV). The electronic states of the C_8-SAMs were evaluated over a wide energy range covering $E_F \pm 6$ eV by employing two types of complementary STS, current−voltage (I−V) and distance−voltage (z−V) measurements at a constant tunneling distance and current, respectively. We observed the electronic states derived from the covalent bonding among the sulfur atom in the thiol group and the surface gold atoms (Au−S bond) near E_F in the standing-up and lying-down phases but not in the lattice-gas phase. Furthermore, at higher and deeper energies than those in which the Au−S-derived states appear, in addition to the electronic states coming from the alkyl chain, empty image potential states were clearly observed on the SAMs at an energetic position correlated with the surface molecular density.

RESULTS AND DISCUSSION

Figure 1a shows an STM image (50 × 43 nm^2) of an as-prepared C_8-SAM taken in a UHV. The surface is composed of multiple domains with a size of at most ~20 nm and vacancy islands with a monatomic depth of Au(111), so-called etch pits.[9,10,27,28] The molecularly resolved STM image reveals that there are two kinds of molecular superstructure, $(\sqrt{3} \times \sqrt{3})R30°$ and c($4\sqrt{3} \times 2\sqrt{3}$)R30°, relative to the underlying Au(111)1 × 1 lattice as shown in Figure 1 panels b and c, respectively. It is widely accepted that they are composed of densely packed alkanethiolates standing in an upright position with a tilt angle of ~30° from the surface normal. In the conventional model, the $\sqrt{3} \times \sqrt{3}$ and c($4\sqrt{3} \times 2\sqrt{3}$) structures are formed by the adsorption of individual alkanethiolates at equivalent and nonequivalent positions, respectively, such as hollow, bridge, or atop sites, on the unreconstructed Au(111) surface.[6−10,19−21] Recently, more feasible models involving Au adatoms, vacancies, and/or Au-alkanethiolate complexes have been proposed for the standing-up phase,[9,10,29,30] although no definitive conclusion has been reached. A tentative model is shown in the Supporting Information.

The geometric structures of alkanethiolate SAMs are controllable by thermal annealing under UHV. In the C_8-SAM prepared by our wet processes, the domain of the c($4\sqrt{3} \times 2\sqrt{3}$) structure mainly appears with a surface coverage of ~90%. This tendency becomes marked after annealing the SAM, as follows. Figure 1 panels d, e, and f show STM images taken on the C_8-SAM after annealing at 70, 120, and 150 °C, respectively. The C_8-SAM annealed at 70 °C is composed of a molecularly flat and extremely large domain with a size

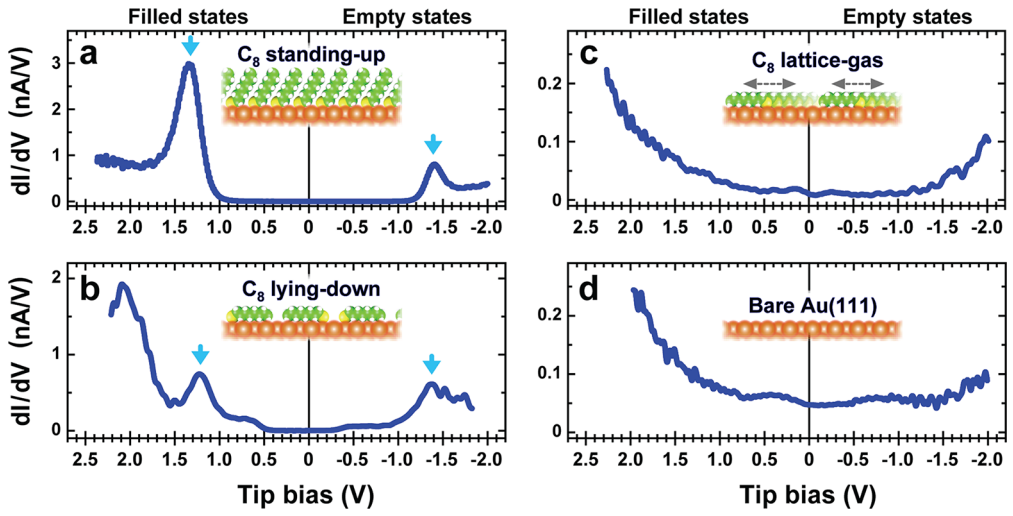

Figure 2. Electronic states of C_8-SAMs evaluated by scanning tunneling $I-V$ spectroscopy. (a, b, c) dI/dV spectra taken on SAMs with standing-up, lying-down, and lattice-gas phases, respectively. (d) dI/dV spectrum taken on Au(111) surface after desorbing C_8 molecules by thermal annealing at 550 °C. Each dI/dV data point was numerically derived from the respective tunneling $I-V$ curve obtained by averaging almost three hundred original curves that were measured within the disabled feedback loop of the STM. The set points of the $I-V$ measurements were V_{tip} = 1.0 V and I_t = 50 pA (a), V_{tip} = 1.0 V and I_t = 200 pA (b), V_{tip} = 1.2 V and I_t = 20 pA (c), and V_{tip} = −1.0 V and I_t = 50 pA (d).

of at least 100 nm as shown in Figure 1d. The observed annihilation of etch pits from the alkanethiolate SAMs agrees with the previous reports; the etch pits in SAMs on Au(111) coalesce to form large vacancy islands or migrate into preexisting substrate steps upon thermal annealing.[27,28] The created large domain is homogeneous with a well-ordered molecular arrangement of the c($4\sqrt{3} \times 2\sqrt{3}$) structure as shown in the high-resolution image (inset in Figure 1d). After annealing at a higher temperature (120 °C), a widely spaced stripe structure is formed as shown in Figure 1e. Each stripe consists of protrusions arranged along the [$11\bar{2}$] direction with a periodicity of $\sqrt{3}a_0$ (0.499 nm), where a_0 is the interatomic distance on the Au(111) surface, as shown in the magnified image (inset in Figure 1e). It has been reported that an alkanethiolate SAM with a stripe structure is composed of flat lying-down adsorbates under the condition of a lower molecular coverage than that of the standing-up phase.[7−10,22,23] This suggests that the transition from the standing-up phase to the lying-down phase occurs *via* partial molecular desorption during thermal annealing at 120 °C. This is supported by the results of previous thermal desorption spectroscopy (TDS) which revealed that the alkanethiolate molecules in SAMs with the standing-up phase partially desorb from the Au(111) surface at 108−120 °C.[31,32] In addition, most of the surface is covered with a two-dimensional molecular lattice-gas phase after annealing at 150 °C, as shown in Figure 1f. In the lattice-gas phase, molecules on the Au(111) surface are rapidly hopping at the time scale of the STM scan owing to a lack of intermolecular interaction,[22,23] indicating that the density of molecules on the surface is decreased by further annealing. The possible chemical species composing the lattice-gas phase are discussed later.

The electronic structures of each phase are evaluated on the basis of STS. Figure 2 panels a and b show dI/dV spectra taken on the C_8-SAMs with the standing-up and lying-down phases, respectively. Each dI/dV datum was numerically differentiated from averaged tunneling $I-V$ curves which were measured on each SAM while keeping the tip height constant with the STM feedback loop disabled. The dI/dV spectra at negative and positive tip bias voltages (V_{tip}) probe the empty and filled states of the sample, respectively. Note that all the STS spectra of the SAM with the standing-up phase were taken on the domains with the c($4\sqrt{3} \times 2\sqrt{3}$) structure. The two d$I$/d$V$ peaks at approximately −1.4 V and +1.3 V are reproducibly observed in both C_8-SAMs as shown in Figure 2a,b. In contrast, these peaks do not appear in the spectra taken on the SAM with the lattice-gas phase (Figure 2c) and the Au(111) surface after removal of the molecules by thermal annealing at 550 °C (Figure 2d). This implies that the observed dI/dV peaks originate from the electronic states of C_8 molecules rigidly adsorbed on the substrate surface. In addition, the electronic states appear within the range of −1.0 to +1.0 V on the lying-down phase but not on the standing-up phase as shown in Figure 2a,b. Since similar electronic states are observed on the bare Au(111) substrate, as shown in Figure 2d, we think that electron tunneling between the STM tip and the substrate occurs across the SAM with the lying-down phase owing to its small thickness compared with that of the standing-up phase. In other words, the alkyl chain and end group make a smaller contribution to the electron tunneling at low bias voltages.

In previous photoemission electron spectroscopy (PES) studies on alkanethiolate SAMs, no noteworthy

electronic states were observed in the energy range within $E_F \pm 3$ eV,[18,33] because alkane molecules have a large energy gap between the HOMO and lowest unoccupied molecular orbital (LUMO) of about 7–12 eV.[24,34–36] In UPS measurements on alkanethiolate SAMs with short alkyl chains, small shoulder-like features were recognized at approximately 1.4 eV below E_F and were attributed to Au–S bonds localized at the molecule–substrate interface.[18] Although little attention has been given to this localized state from the viewpoint of electrical conduction through the molecule, our result clearly indicates that this state plays a significant role in electron conduction at low bias voltages, and is in good agreement with the average tunneling barrier height extracted from I–V measurement.[15–17] Interestingly, the electronic states discussed here are not observed in the lattice-gas phase as mentioned above. This suggests that a rigid chemical bond is not formed between the thiol terminal and the Au(111) surface in the lattice-gas phase.

Although the chemical species composing the lattice-gas phase are still controversial, our STM observation indicates that the diffusing species in the lattice-gas phase maintain the moieties of the original alkanethiolates such as the end group, alkyl chain, and sulfur atom (see Supporting Information). One of the possible candidates are dimers of alkanethiolates [$CH_3(CH_2)_7S$–$S(CH_2)_7CH_3$] formed after the breaking of Au–S bonds. These dimers would weakly interact with the Au(111) surface and diffuse on the surface without forming Au–S bonds. On the other hand, there is a possibility that the lattice-gas phase is composed of individual alkanethiolates [$CH_3(CH_2)_7S$–], because previous theoretical studies have revealed that the energy barrier for the diffusion of isolated alkanethiolates on a Au(111) surface is sufficiently small to allow their diffusion at room temperature (RT).[37,38] In this case, since the formation and cleavage of chemical bonds between the diffused species and the substrate surface frequently occur, it would be difficult to clearly detect the electronic states derived from the Au–S bonds in STS measurements. Detailed identification of the molecular species in the lattice-gas phase and the clarification of their electronic structure are expected to be possible by performing STM/STS experiments at a low temperature to suppress molecular diffusion.

We also evaluate the electronic states at higher and deeper energies than those in which the Au–S-derived states appear. Note that reliable tunneling I–V spectroscopy has seldom been achieved under a bias voltage larger than ~3 V at RT because of the destruction of the tip apex and/or the SAMs induced by the large increases in the electric field and current density in the tunneling junction. To overcome these difficulties, we carried out tunneling z–V spectroscopy, in which the change in the tip height is measured during voltage sweeps while maintaining a constant tunneling current (I_t).[39,40] In this

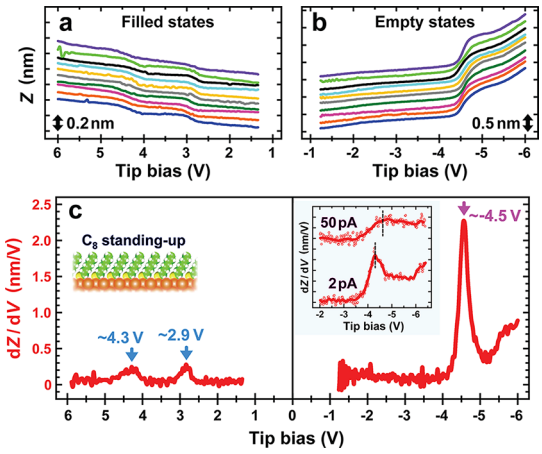

Figure 3. Electronic states of C_8-SAMs evaluated by scanning tunneling z–V spectroscopy. (a and b) Series of 10 z–V curves continuously taken at different positions on the SAM with the standing-up phase to evaluate its filled and empty states, respectively. The tunneling current was kept to constant values of I_t = 5 pA and 2 pA while obtaining spectra a and b, respectively. (c) dz/dV spectra showing filled and empty states of the C_8-SAM, which were obtained by numerically deriving the averaged z–V curves in panels a and b, respectively. The inset in panel c shows dz/dV spectra of the SAM taken under the feedback conditions of I_t = 50 pA (upper) and 2 pA (lower).

spectroscopy, the STM tip retracts away from the sample surface when the bias voltage is increased owing to the feedback of the constant I_t. When the bias voltage is scanned through the electronic states of the sample, the tip retraction drastically increases, resulting in a step-shaped feature appearing in the measured z–V curve. This method enables us to perform tunneling spectroscopy at larger bias voltages with little risk of destruction of the tip apex and sample, because the increases in the electric field and current density in the tunneling junction are moderated by setting the current set point as small as possible. Note that the sensitivity of tunneling z–V spectroscopy under the suppressed current set point is low compared with that of the conventional I–V spectroscopy, although a major advantage of tunneling z–V spectroscopy is a wider accessible bias range, particularly for delicate samples.

Figure 3 panels a and b show z–V curves measured on the standing-up phase of the C_8-SAM by sweeping V_{tip} from +1.3 to +6.0 V at an I_t of 5 pA and from −1.2 to −6 V at an I_t of 2 pA, respectively. Each series of 10 z–V curves was continuously acquired at different positions on the surface by interrupting an image scan. Stepwise retractions of the STM tip reproducibly appear at the same voltages. This indicates that resonant tunneling through the electronic states of the SAM occurs at these voltages. The energetic positions of the electronic states are more clearly recognized in the dz/dV plots (Figure 3c), which were obtained by numerically differentiating the z–V curve formed by averaging the 10 curves shown in Figure 3a,b. In the empty states, a

single dz/dV peak with a high intensity is observed at −4.5 V, while two weak peaks appear at +2.9 V and +4.3 V in the filled-state spectrum.

Regarding the filled states of alkanethiols bound with a gold surface, density functional calculations have revealed that the delocalized state along the alkyl chain appear at 3−4 eV below E_F, which is directly related to the HOMO of the pure alkane.[24] These states are expected to be the main conductance channels through the molecule at higher voltages, and can be detected by z−V spectroscopy as demonstrated in the present study. On the other hand, the Au−S-derived states observed at $E_F \pm \sim$1.5 eV cannot be recognized in the dz/dV spectra, as shown in Figure 3c, since they are localized at the buried interface and contribute less to the tunneling conductance than the alkyl-chain-derived states.

Turning to the empty state, one can clearly observe a sharp dz/dV peak at −4.5 V. Its significantly high intensity implies that it is considerably different from the filled-state peaks in its essential characteristic. A possible candidate for this peak is the first (n = 1) image potential state (IPS). The IPS comprises the hydrogenic series of electronic states formed by the image charges of electrons existed on the solid surface.[39] The IPSs appear at an energy of at most ∼0.85 eV below the vacuum level and can be easily accessed by STS because they have a maximum probability density in the vacuum gap.[41,42] In previous two-photon photoemission experiments, the first IPSs formed on alkanethiolate SAMs were observed at 3.7−4.2 eV above E_F.[34,43,44] In the STS experiment, since the strong electric field beneath the STM tip distorts the Coulomb potential formed in the tunneling gap by image charges, the energy levels of IPSs shift to higher than that of the zero field, which is called the Stark shift.[39,41] We investigated the effect of the electric field on the observed dz/dV peak by changing the set point of I_t. The inset in Figure 3c shows two dz/dV spectra taken under the set points of I_t = 50 pA (upper) and I_t = 2 pA (lower), namely, the upper spectrum was taken under a larger electric field in the tunneling gap than the lower spectrum. The energetic position of the dz/dV peak certainly shifts toward a higher energy upon increasing the magnitude of the electric field, as expected. Therefore, the observed empty state can be safely attributed to the Stark-shifted first IPS.

We also investigated the IPSs formed on other phases of the C_8-SAM. Figure 4a,b, and 4c show typical empty-state dz/dV spectra taken on SAMs with the standing-up, lying-down, and lattice-gas phases, respectively. The typical spectrum of each SAM was determined on the basis of statistical analysis using more than two thousand z−V curves. The strong peak at −4.5 V in the dz/dV spectrum of the standing-up SAM (Figure 4a) is considered to originate from the first IPS, as mentioned above, whereas the spectra taken on

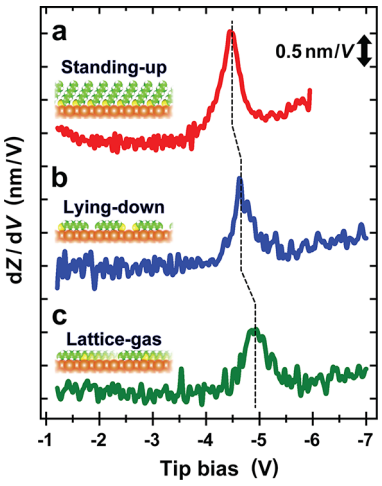

Figure 4. Empty-state dz/dV spectra taken on the C_8-SAMs with (a) standing-up, (b) lying-down, and (c) lattice-gas phases. During z−V measurements, the tunneling current was kept constant at I_t = 2 pA, 4 pA, and 5 pA while obtaining spectra a, b, and c, respectively.

the lying-down and lattice-gas phases show peaks at larger bias voltages of −4.6 and −4.9 V as shown in Figure 4b,c, respectively. These spectra are obviously different from that of the first IPS taken on a clean Au(111) surface, in which a broad dz/dV peak appears at ∼5.5 eV above E_F,[39] indicating that the observed dz/dV peaks certainly originate from the C_8-SAMs. In contrast to the Au−S-derived states near E_F shown in Figure 2, the IPS is observed not only on the standing-up and lying-down phases but also on the lattice-gas phase. This is consistent with the fact that the IPSs are formed on flat surfaces regardless of the formation of chemical bonds between the adsorbates and substrate, because the IPS arises from the Coulomb interaction between electrons on the surface and its positive image charges formed by the polarization of the nearby conduction band electrons.[39,41,42]

As can be seen from Figure 4, the energetic position of the IPS is slightly different between each phase of the SAM. Since IPSs are pinned to the vacuum level of the substrate, their energetic positions are sensitive to changes in the work function of the surface. It has been reported that the work function of a bare Au(111) surface (5.55 eV) is decreased by forming hexanethiol SAMs with lying-down (4.6 eV) and standing-up (4.3 eV) phases,[43] which is consistent with the energetic shift of the IPS observed in the present study. When organic molecules are adsorbed on solid surfaces, it is known that the induced dipole moment in the adsorbates generally lowers the work function of the surface, which is enhanced by increasing the density of the adsorbates.[45] In the present case, each phase of the SAM has a different molecular density because it was formed *via* molecule desorption by thermal annealing. Therefore, the observed upward energy shift of the IPS upon changing the geometry from the standing-up

phase to the lattice-gas phase through the lying-down phase can be attributed to the change in the surface potential energy which is correlated with the restoration of the work function of the Au(111) surface.

CONCLUSIONS

The electronic structures of alkanethiolate SAMs composed of wide domains with standing-up, lying-down, and lattice-gas phases were precisely investigated by STM/STS with an energy range of $E_F \pm 6$ eV. We demonstrated that the combination of tunneling $z-V$ and $I-V$ spectroscopy is useful for evaluating the electronic properties of thin films of organic molecules with a wide energy range and molecular-scale spatial resolution. We believe that the present results will provide insights toward precise control of the injection, separation, and storage of charge carriers in alkanethiolate SAMs and their derivatives formed on metal surfaces.

EXPERIMENTAL METHODS

SAMs of octanethiol [$CH_3(CH)_7SH$] were formed from liquid phases onto single-crystal Au(111) substrates. The substrates were cleaned by repeated cycles of sputtering with 0.6 keV Ar^+ ions followed by annealing at 450 °C in a UHV prior to the formation of SAMs. The alkanethiolate SAMs were prepared by dipping the substrate into ethanol solution including alkanethiol molecules with a concentration of 12.5 mM at RT for 20 h. The dipped substrate was rinsed thoroughly with ethanol and dried in air at atmospheric pressure. All STM/STS experiments were performed at RT in a custom-built UHV chamber with a base pressure lower than 1.0×10^{-8} Pa, which houses a commercial STM unit (Omicron VT-AFM-XA50/500). We used electrochemically etched W wires for the STM/STS probe. STM images were analyzed using WSxM.[46]

Conflict of Interest: The authors declare no competing financial interest.

Supporting Information Available: Additional data and discussion about the present C_8-SAM with standing-up and lattice-gas phases. This material is available free of charge *via* the Internet at http://pubs.acs.org.

REFERENCES AND NOTES

1. Joachim, C.; Gimzewski, J. K.; Aviram, A. Electronics Using Hybrid-Molecular and Mono-Molecular Devices. *Nature* **2000**, *408*, 541–548.
2. Donhauser, Z. J.; Mantooth, B. A.; Kelly, K. F.; Bumm, L. A.; Monnell, J. D.; Stapleton, J. J.; Price, D. W., Jr.; Rawlett, A. M.; Allara, D. L.; Tour, J. M.; *et al.* Conductance Switching in Single Molecules through Conformational Changes. *Science* **2001**, *292*, 2303–2307.
3. Chen, J.; Reed, M. A.; Rawlett, A. M.; Tour, J. M. Large On−Off Ratios and Negative Differential Resistance in a Molecular Electronic Device. *Science* **1999**, *286*, 1550–1552.
4. Barth, J. V.; Costantini, G.; Kern, K. Engineering Atomic and Molecular Nanostructures at Surfaces. *Nature* **2005**, *437*, 671–679.
5. Claridge, S. A.; Castleman, A. W., Jr.; Khanna, S. N.; Murray, C. B.; Sen, A.; Weiss, P. S. Cluster-Assembled Materials. *ACS Nano* **2009**, *3*, 244–255.
6. Ulman, A. Formation and Structure of Self-Assembled Monolayers. *Chem. Rev.* **1996**, *96*, 1533–1554.
7. Schreiber, F. Structure and Growth of Self-Assembling Monolayers. *Prog. Surf. Sci.* **2000**, *65*, 151–256.
8. Love, J. C.; Estroff, L. A.; Kriebel, J. K.; Nuzzo, R. G.; Whitesides, G. M. Self-Assembled Monolayers of Thiolates on Metals as a Form of Nanotechnology. *Chem. Rev.* **2005**, *105*, 1103–1169.
9. Maksymovych, P.; Voznyy, O.; Dougherty, D. B.; Sorescu, D. C.; Yates, J. T., Jr. Gold Adatom as a Key Structural Component in Self-Assembled Monolayers of Organosulfur Molecules on Au(1 1 1). *Prog. Surf. Sci.* **2010**, *85*, 206–240.
10. Vericat, C.; Vela, M. E.; Benitez, G.; Carro, P.; Salvarezza, R. C. Self-Assembled Monolayers of Thiols and Dithiols on Gold: New Challenges for a Well-Known System. *Chem. Soc. Rev.* **2010**, *39*, 1805–1834.
11. Kumar, A.; Whitesides, G. M. Patterned Condensation Figures as Optical Diffraction Gratings. *Science* **1994**, *263*, 60–62.
12. Uosaki, K.; Kondo, T.; Zhang, X. Q.; Yanagida, M. Very Efficient Visible-Light-Induced Uphill Electron Transfer at a Self-Assembled Monolayer with a Porphyrin−Ferrocene−Thiol Linked Molecule. *J. Am. Chem. Soc.* **1997**, *119*, 8367–8368.
13. Shon, Y. S.; Kelly, K. F.; Halas, N. J.; Lee, T. R. Fullerene-Terminated Alkanethiolate SAMs on Gold Generated from Unsymmetrical Disulfides. *Langmuir* **1999**, *15*, 5329–5332.
14. Nagaoka, S.; Ikemoto, K.; Horiuchi, K.; Nakajima, A. Soft- and Reactive-Landing of $Cr(aniline)_2$ Sandwich Complexes onto Self-Assembled Monolayers: Separation between Functional and Binding Sites. *J. Am. Chem. Soc.* **2011**, *133*, 18719–18727.
15. Cui, X. D.; Zarate, X.; Tomfohr, J.; Sankey, O. F.; Primak, A.; Moore, A. L.; Moore, T. A.; Gust, D.; Harris, G.; Lindsay, S. M. Making Electrical Contacts to Molecular Monolayers. *Nanotechnology* **2002**, *13*, 5–14.
16. Wang, W. Y.; Lee, T.; Reed, M. A. Mechanism of Electron Conduction in Self-Assembled Alkanethiol Monolayer Devices. *Phys. Rev. B* **2003**, *68*, 035416.
17. Engelkes, V. B.; Beebe, J. M.; Frisbie, C. D. Length-Dependent Transport in Molecular Junctions Based on SAMs of Alkanethiols and Alkanedithiols: Effect of Metal Work Function and Applied Bias on Tunneling Efficiency and Contact Resistance. *J. Am. Chem. Soc.* **2004**, *126*, 14287–14296.
18. Alloway, D. M.; Hofmann, M.; Smith, D. L.; Gruhn, N. E.; Graham, A. L.; Colorado, R., Jr.; Wysocki, V. H.; Lee, T. R.; Lee, P. A.; Armstrong, N. R. Interface Dipoles Arising from Self-Assembled Monolayers on Gold: UV-Photoemission Studies of Alkanethiols and Partially Fluorinated Alkanethiols. *J. Phys. Chem. B* **2003**, *107*, 11690–11699.
19. Widrig, C. A.; Alves, C. A.; Porter, M. D. Scanning Tunneling Microscopy of Ethanethiolate and *n*-Octadecanethiolate Monolayers Spontaneously Adsorbed at Gold Surfaces. *J. Am. Chem. Soc.* **1991**, *113*, 2805–2810.
20. Poirier, G. E.; Tarlov, M. J. The c(4 × 2) Superlattice of *n*-Alkanethiol Monolayers Self-Assembled on Au(111). *Langmuir* **1994**, *10*, 2853–2856.
21. Noh, J.; Kato, H. S.; Kawai, M.; Hara, M. Surface Structure and Interface Dynamics of Alkanethiol Self-Assembled Monolayers on Au(111). *J. Phys. Chem. B* **2006**, *110*, 2793–2797.
22. Poirier, G. E.; Pylant, E. D. The Self-Assembly Mechanism of Alkanethiols on Au(111). *Science* **1996**, *272*, 1145–1148.
23. Poirier, G. E. Coverage-Dependent Phases and Phase Stability of Decanethiol on Au(111). *Langmuir* **1999**, *15*, 1167–1175.
24. Seminario, J. M.; Yan, L. *Ab Initio* Analysis of Electron Currents in Thioalkanes. *Int. J. Quantum Chem.* **2005**, *102*, 711–723.
25. Sun, Q.; Selloni, A. Interface and Molecular Electronic Structure *vs* Tunneling Characteristics of CH_3- and CF_3-Terminated Thiol Monolayers on Au(111). *J. Phys. Chem. A* **2006**, *110*, 11396–11400.
26. Toher, C.; Rungger, I.; Sanvito, S. Simulating STM Transport in Alkanes from First Principles. *Phys. Rev. B* **2009**, *79*, 205427.

27. McCarley, R. L.; Dunaway, D. J.; Willicut, R. J. Mobility of the Alkanethiol−Gold(111) Interface Studied by Scanning Probe Microscopy. *Langmuir* **1993**, *9*, 2775–2777.
28. Bucher, J. P.; Santesson, L.; Kern, K. Thermal Healing of Self-Assembled Organic Monolayers: Hexane- and Octadecanethiol on Au(111) and Ag(111). *Langmuir* **1994**, *10*, 979–983.
29. Häkkinen, H. The Gold-Sulfur Interface at the Nanoscale. *Nat. Chem.* **2012**, *4*, 443–455.
30. Voznyy, O.; Dubowski, J. J. *c*(4 × 2) Structures of Alkanethiol Monolayers on Au (111) Compatible with the Constraint of Dense Packing. *Langmuir* **2009**, *25*, 7353–7358.
31. Stettner, J.; Winkler, A. Characterization of Alkanethiol Self-Assembled Monolayers on Gold by Thermal Desorption Spectroscopy. *Langmuir* **2010**, *26*, 9659–9665.
32. Hayashi, T.; Wakamatsu, K.; Ito, E.; Hara, M. Effect of Steric Hindrance on Desorption Processes of Alkanethiols on Au(111). *J. Phys. Chem. C* **2009**, *113*, 18795–18799.
33. Qi, Y.; Yaffe, O.; Tirosh, E.; Vilan, A.; Cahen, D.; Kahn, A. Filled and Empty States of Alkanethiol Monolayer on Au (111): Fermi Level Asymmetry and Implications for Electron Transport. *Chem. Phys. Lett.* **2011**, *511*, 344–347.
34. Muntwiler, M.; Lindstrom, C. D.; Zhu, X. Y. Delocalized Electron Resonance at the Alkanethiolate Self-Assembled Monolayer/Au(111) Interface. *J. Chem. Phys.* **2006**, *124*, 081104.
35. Tomfohr, J. K.; Sankey, O. F. Complex Band Structure, Decay Lengths, and Fermi Level Alignment in Simple Molecular Electronic Systems. *Phys. Rev. B* **2002**, *65*, 245105.
36. Salomon, A.; Cahen, D.; Lindsay, S.; Tomfohr, J.; Engelkes, V. B.; Frisbie, C. D. Comparison of Electronic Transport Measurements on Organic Molecules. *Adv. Mater.* **2003**, *15*, 1881–1890.
37. Franke, A.; Pehlke, E. Adsorption and Diffusion of SCH_3 Radicals and $Au(SCH_3)_2$ Complexes on the Unreconstructed Au(111) Surface in the Submonolayer Coverage Regime. *Phys. Rev. B* **2009**, *79*, 235441.
38. Jiang, D.; Dai, S. Diffusion of the Linear CH_3S-Au-SCH_3 Complex on Au(111) from First Principles. *J. Phys. Chem. C* **2009**, *113*, 3763–3766.
39. Dougherty, D. B.; Maksymovych, P.; Lee, J.; Feng, M.; Petek, H.; Yates, J. T., Jr. Tunneling Spectroscopy of Stark-Shifted Image Potential States on Cu and Au Surfaces. *Phys. Rev. B* **2007**, *76*, 125428.
40. Pronschinske, A.; Mardit, D. J.; Dougherty, D. B. Modeling the Constant-Current Distance−Voltage Mode of Scanning Tunneling Spectroscopy. *Phys. Rev. B* **2011**, *84*, 205427.
41. Binnig, G.; Frank, K. H.; Fuchs, H.; Garcia, N.; Reihl, B.; Rohrer, H.; Salvan, F.; Williams, A. R. Tunneling Spectroscopy and Inverse Photoemission: Image and Field States. *Phys. Rev. Lett.* **1985**, *55*, 991–994.
42. Güdde, J.; Höfer., U. Femtosecond Time-Resolved Studies of Image Potential States at Surfaces and Interfaces of Rare-Gas Adlayers. *Prog. Surf. Sci.* **2005**, *80*, 49–91.
43. Lindstrom, C. D.; Muntwiler, M; Zhu, X. Y. Electron Transport Across the Alkanethiol Self-Assembled Monolayer/Au(111) Interface: Role of the Chemical Anchor. *J. Phys. Chem. B* **2005**, *109*, 21492–21495.
44. Shibuta, M.; Hirata, N.; Matsui, R.; Eguchi, T.; Nakajima, A. Charge Separation at the Molecular Monolayer Surface: Observation and Control of the Dynamics. *J. Phys. Chem. Lett.* **2012**, *3*, 981–985.
45. Dougherty, D. B.; Maksymovych, P.; Lee, J.; Yates, J. T., Jr. Local Spectroscopy of Image-Potential-Derived States: From Single Molecules to Monolayers of Benzene on Cu(111). *Phys. Rev. Lett.* **2006**, *97*, 236806.
46. Horcas, I.; Fernández, R.; Gómez-Rodríguez, J. M.; Colchero, J.; Gómez-Herrero, J.; Baro, A. M. WSxM: A Software for Scanning Probe Microscopy and a Tool for Nanotechnology. *Rev. Sci. Instrum.* **2007**, *78*, 013705.